Journal of Applied Polymer Science

Dithieno[2,3-d:2′,3′-d′]naphtho[2,1-b:3,4-b′]dithiophene based medium bandgap conjugated polymers for photovoltaic applications

Chunyan Yang,[1] Huijuan Li,[2] Junfeng Tong,[1] Jianfeng Li,[1] Peng Zhang,[1] Yangjun Xia[1]

[1]Key Lab of Optoelectronic Technology and Intelligent Control of Education Ministry, Lanzhou Jiaotong University, Lanzhou 730000, China

[2]College of Chemical and Biological Engineering, Lanzhou Jiaotong University, Lanzhou 730000, China

Correspondence to: Y. Xia (E-mail: yjxia73@126.com)

ABSTRACT: Three novel medium band gap (MBG) conjugated polymers (CPs) (named as P1, P2, and P3, respectively) were developed by copolymerizing 2,7-dibromo-10,11-di(2-hexyldecyloxy)dithieno[2,3-d:2′,3′-d′]naphtho[2,1-b:3,4-b′]dithiophene (NDT-Br) with three different units: 2,5-bis(tributylstannyl)thiophene, 2,5-bis(trimethylstannyl)thieno[3,2-b]thiophene and *trans*−1,2-bis(tributylstannyl)ethene, respectively. The thermal, optical, and electrochemical properties of the polymers were investigated. All of the polymers have good thermal stability and medium band gap (∼ 1.9 eV). Prototype bulk heterojunction photovoltaic cells based on the blend P1/P2/P3 and [6, 6] phenyl-C61 butyric acid methyl ester ($PC_{61}BM$) were assembled and the photovoltaic properties were assessed. Power conversion efficiencies (PCEs) of 1.61% ∼ 2.43% have been obtained under 100 mW cm^{-2} illumination (AM1.5). © 2016 Wiley Periodicals, Inc. J. Appl. Polym. Sci. **2016**, *133*, 43288.

KEYWORDS: applications; optical and photovoltaic applications; properties and characterization

Received 2 May 2015; accepted 29 November 2015

DOI: 10.1002/app.43288

INTRODUCTION

Recently, polycyclic thienoacenes with larger coplanar core and more extended conjugation length are complimented by an extensive set of advantageous characteristics, such as enhanced charge-carrier mobilities, decreased band gaps, effective exciton separation into free charge carriers of the corresponding conjugated polymers (CPs), all of which are essential to achieve high device performance.[1–10] For example, in 2010, You and coworkers prepared a donor–acceptor polymer (PQTN-BT) based on quadrathienonaphthalene (QTN), and the polymer showed a PCE over 2% in corresponding polymer solar cells (PSCs).[3] Subsequently, Yu and coworkers synthesized a series of CPs (PTAT-x) containing extended π-conjugated tetrathienoanthracene units in 2011. The polymer PTAT-3 with 2-butyloctyl alkyl side chains exhibited a PCE about 5.6% with [6,6] phenyl-C61 butyric acid methyl ester ($PC_{61}BM$).[4] Furthermore, Hou and coworkers prepared a CP (PDTT) based on 5,10-di(2-hexyldecyloxy)dithieno[2,3-d:2′,3′-d′]benzo[1,2-b:4,5-b′]dithiophene (DTBDT) and obtained a PCE of 3.64% in corresponding PSCs.[5] Lately, with DTBDT as the electron donor and 2,1,3-benzothiadiazole as the electron acceptor, Kwon and coworkers synthesized a CP (PDTBDAT-BZ), and received a PCE of 5.1% based on the CP.[6] In addition, Yu and coworkers presented a series of CPs based on dithieno[2,3-d:2′,3′-d′]benzo[1,2-b:4,5-b′]dithiophene (DBD), the PCEs of 3.9 ∼ 7.6% have been achieved in the PSCs from the CPs.[7] Our group also prepared a new CP named as PNDT-BT based on a novel hexacyclic thienoacene derivative 10,11-di(3,7-dimethyloctyloxy)dithieno[2,3-d:2′,3′-d′]naphtho[2,1-b:3,4-b′]dithiophene (NDT).[8] Moreover, other novel thienoacene derivatives such as naphtho[2,1-b:3,4-b′]dithiophene,[9] anthradithiophene[10] etc., have also been developed and used as electron-rich building blocks for high performance CPs. Evidently, most of the polymers based on polycyclic thienoacenes exhibit high hole mobility, low band gap, and notably high performance in the PSCs.

Although low band gap (LBG) CPs receive a great deal of attention owing to their great success in PSCs, the exploration of medium band gap (MBG) CPs with good photovoltaic properties was seemingly overlooked. Virtually, the work of developing MBG CPs is also of great importance. It is well known that though PCE over 9% has been reported in single junction devices,[11] this efficiency is far away from the commercialization of PSCs. One of the key reasons is the narrow absorption range of single donor polymer, which limits the use of the full solar spectrum. In order to use solar radiation more effectively,

Additional Supporting Information may be found in the online version of this article.

© 2016 Wiley Periodicals, Inc.

assembly of tandem PSCs has been demonstrated to be a successful approach,[12–15] as multiple photoactive layers with matched and complementary absorption spectra are stacked in series in tandem PSCs. That is, in a tandem PSCs, there are two cells connected in series through an interconnecting layer: the front cell and the rear cell. The front cell is made by MBG materials, which convert higher energy photons, while the rear cell is made by LBG materials, which absorb the lower energy photons. So far, most researches carried out on tandem PSCs have focused on development of new LBG conjugated polymers CPs (absorb in the range of 700 ∼ 1000 nm) to use in the rear cell.[15–18] However, the MBG CPs (absorb in the range of 400 ∼ 700 nm) with good photovoltaic properties that employed in the front cell is almost poly(3-hexylthiophene) (P3HT). Therefore, except P3HT, exploration of other MBG conjugated materials with good photovoltaic properties is extremely important.[19–32]

Herein, based on our previous work,[8] we developed three novel MBG CPs (named as P1, P2, and P3, respectively) by copolymerizing 2,7-dibromo-10,11-di(2-hexyldecyloxy)dithieno[2,3-d:2′,3′-d′]naphtho[2,1-b:3,4-b′]dithiophene (NDT-Br) with 2,5-bis(tributylstannyl)thiophene/2,5-bis(trimethylstannyl)-thieno[3,2-b]thiophene/*trans*-1,2-bis(tributylstannyl)ethene, respectively. The optical, electrochemical, and photovoltaic properties of the polymers were investigated in details. These polymers absorb in the range of 340 ∼ 650 nm with a band gap of about 1.9 eV. Prototype bulk heterojunction photovoltaic cells based on the blend P1, P2, P3, and $PC_{61}BM$, show PCEs up to 1.61% ∼ 2.43% under 100 mW cm^{-2} illumination (AM 1.5). These preliminary results indicate that these MBG conjugated polymers are promising candidates of P3HT for PSCs and deserve to be studied further.

EXPERIMENTAL

Materials

Unless otherwise specified, all reagents were obtained from Aldrich, Acros, TCI Chemical Co. and Shanghai Sinopharm Chemical Reagent Co., and used as received. All the solvents were further purified under a nitrogen flow.

General Methods

^1H NMR spectra were recorded using a Bruker DRX 400 spectrometer operating at 400 MHz with tetramethylsilane (TMS) as reference. The molecular weight of the polymers was measured by the analytical gel permeation chromatography (GPC) method on a Waters GPC 2410 in tetrahydrofuran (THF) via a calibration curve of polystyrene standard. Thermogravimetric analysis (TGA) measurements were performed on a TGA 2050 (TA instruments) thermal analysis system under a heating rate of 10°C min^{-1} and a nitrogen flow rate of 20 mL min^{-1}. UV-visible absorption spectra were taken on a UV-2550 spectrophotometer (Shimadzu). Photoluminescence (PL) spectra were taken by 970 CRT spectrofluorometer (Sanco, Shanghai). Cyclic voltammetry (CV) experiments were conducted on a CHI 660 electrochemical workstation (Shanghai Chenhua Co.) at a scan rate of 50 mV s^{-1} in a nitrogen-saturated solution of acetonitrile containing 0.1 M tetrabutylammonium hexafluorophosphate (Bu_4NPF_6) with polymer films on platinum electrode and Ag/AgCl electrode as the working and reference electrodes, respectively. Tapping-mode atomic force microscopy (AFM) images were obtained using an Agilent 5500 system. The low-resolution TEM images were obtained on a Hitachi HT 7700 microscope, operating at 120 kV.

Fabrication and Characterization of PSCs

Polymer solar cells with device configuration of glass/indium tin oxide (ITO)/poly(3,4-ethylene-dioxythiophene):poly(styrene sulfonate) (PEDOT : PSS)/Polymer: $PC_{61}BM$/Ca/Al were fabricated as follows: a patterned ITO coated glass with a sheet resistance of 10 ∼ 15 Ω $square^{-1}$ was cleaned firstly in de-ionized water, acetone, and isopropanol in turn, then by oxygen plasma treatment for 5 min. After that, a 40 nm thick poly PEDOT : PSS (Bayer Baytron 4083) anode buffer layer was spin-casted onto the ITO substrate and then dried by baking in a vacuum oven at 150// °C for 30 min. The active layer, with a thickness in the 70 ∼ 80 nm range, was then deposited on top of the PEDOT : PSS layer, by spin-casting from an o-dichlorobenzene solution containing P1 : $PC_{61}BM$ (w : w; 1:1, 1:2, 1:3), P2 : $PC_{61}BM$ (w : w; 1:1, 1:2, 1:3), and P3 : $PC_{61}BM$ (w : w; 1:1, 1:2, 1:3), respectively. The thickness of the PEDOT : PSS and active layer were verified by a surface profilometer (DektakXT, Boyue In. Co.). Finally, the 8 nm thickness of calcium and 100 nm thickness of aluminum layer were thermally evaporated with a shadow mask under vacuum of 3×10^{-5} Pa. The thickness of the evaporated cathode was monitored by a quartz crystal thickness/ratio monitor (SI-TM206, Shenyang Sciens Co.). In addition, each device had an active area of 0.10 mm^2. Except for the deposition of the PEDOT : PSS layers, all the fabrication processes were carried out inside a controlled atmosphere in a nitrogen drybox (Etelux Co.) containing less than 1 ppm oxygen and moisture. The PCEs of the resulting polymer solar cells were measured under 1 sun, AM 1.5G (Air mass 1.5 global) condition using a solar simulator (XES-70S1, San-EI Electric Co.) (100 mW cm^{-2}). The current density–voltage (J–V) characteristics were recorded with a Keithley 2410 source-measurement unit in the nitrogen drybox (Etelux Co.). The spectral responses of the devices were measured with a commercial EQE/incident photon to charge carrier efficiency (IPCE) setup (7-SCSpecIII, Beijing 7-star Optical Instruments Co., Ltd.). A calibrated silicon detector was used to determine the absolute photosensitivity.

RESULTS AND DISCUSSION

Synthesis and Structural Characterization of the Monomers and Polymers

As depicted in Scheme 1, monomer 10,11-di(2-hexyldecyloxy)-dithieno[2,3-d:2′,3′-d′]naphtho[2,1-b:3,4-b′]dithiophene (NDT) was synthesized according the procedure described in our previous work.[8] The detailed synthesis procedures and ^1H NMR spectra (Supporting Information Figure S1) of NDT were described in the Supporting Information. Subsequently, NDT was brominated by *N*-bromosuccinimide (NBS) to afford 2,7-dibromo-10,11-di(2-hexyldecyloxy)dithieno[2,3-d:2′,3′-d′]naphtho [2,1-b:3,4-b′]dithiophene (NDT-Br) with a yield of 94%. The chemical structure of NDT-Br was confirmed by ^1H NMR spectra (Supporting Information Figure S2). Finally, NDT-Br was polymerized with 2,5-bis(tributylstannyl)thiophene/2,5-bis(trimethylstannyl)thieno[3,2-b]thiophene/*trans*−1,2-bis

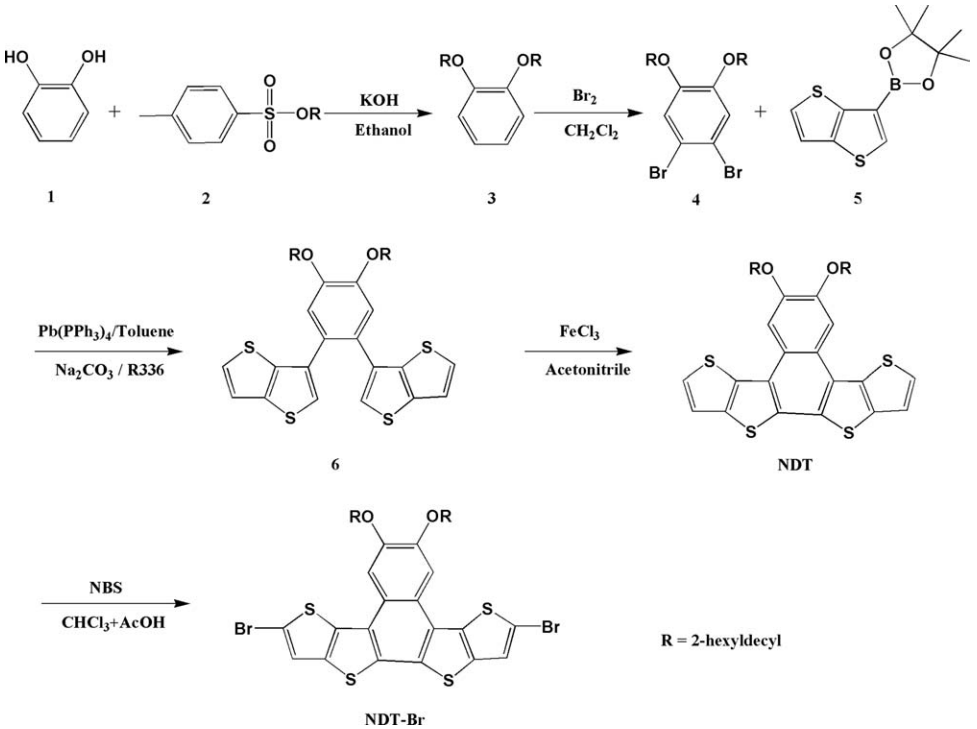

Scheme 1. Synthetic route for the monomer.

(tributylstannyl)ethene by the Stille polycondensation reaction, which was displayed in Scheme 2, to yield the designed polymers-**P1**(the yield of 75%)/**P2** (the yield of 82%)/**P3** (the yield of 65%). All of the polymers are soluble in common organic solvents, such as chloroform, chlorobenzene, and dichlorobenzene. The number-average molecular weights (M_n) of the **P1**, **P2**, and **P3** are 17.8 kDa, 16.2 kDa, and 11.2 kDa with polydispersity index (PDI) of 1.41, 1.63,

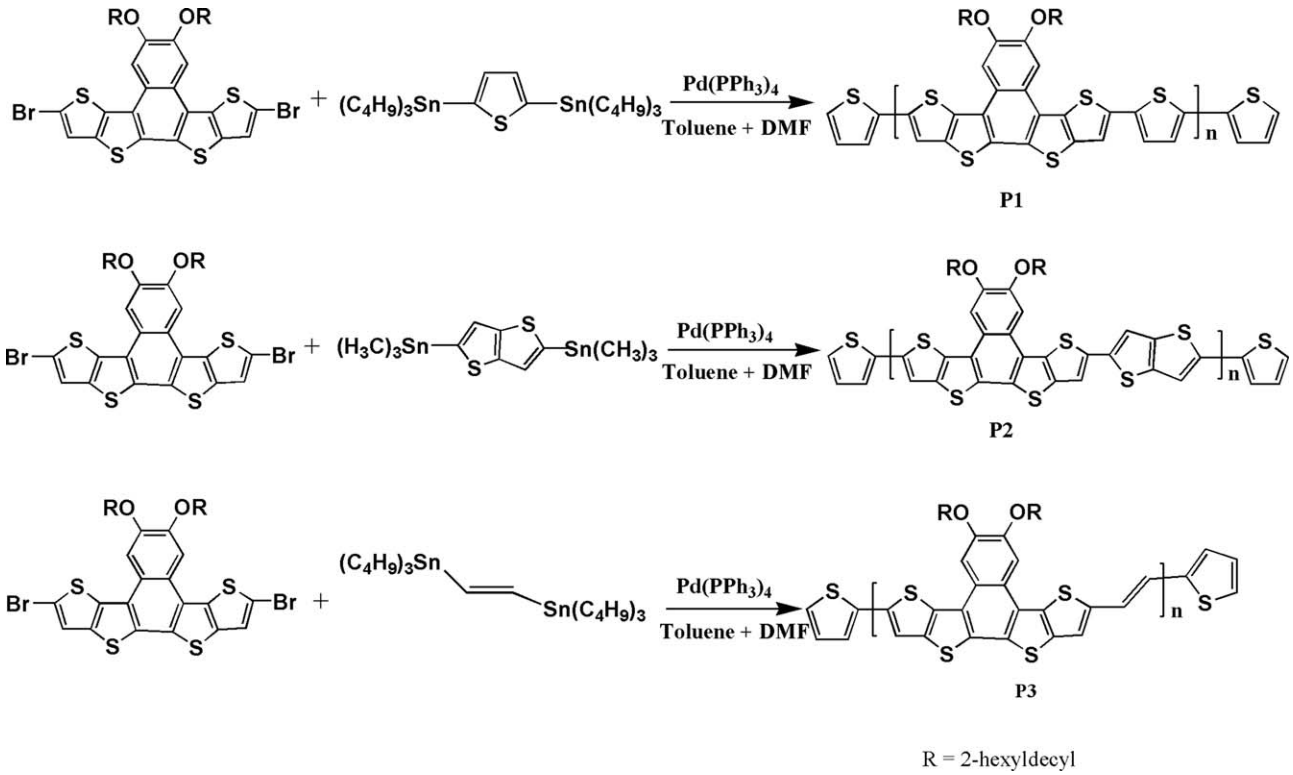

Scheme 2. Synthetic routes for P1, P2, and P3.

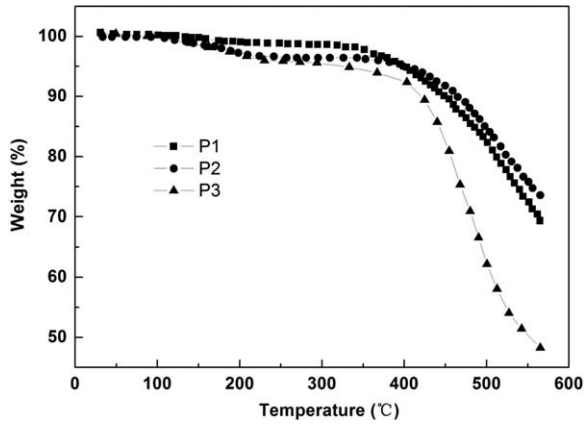

Figure 1. TGA plots of P1, P2, and P3.

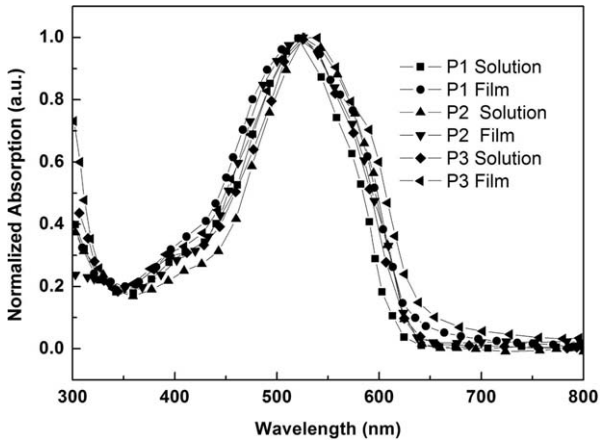

Figure 2. Normalized absorption spectra of P1, P2, and P3 as a film and in toluene solution, respectively.

and 1.86, respectively. The chemical structures of the compounds 10,11-di(2-hexyldecyloxy)dithieno[2,3-d:2′,3′-d′]naphtho[2,1-b:3,4-b′]dithiophene (NDT) and 2,7-dibromo-10,11-di(2-hexyldecyloxy)dithieno[2,3-d:2′,3′-d′]naphtho[2,1-b:3,4-b′]dithiophene (NDT-Br) were confirmed by ^{1}H NMR which were shown in Supporting Information Figures S1 and S2.

Thermal Properties of the Polymers

Thermal stability of the polymers was investigated by thermogravimetric analysis (TGA). The TGA plots were shown in Figure 1. The temperature at 5% weight loss was selected as the onset point of decomposition. All of the polymers exhibited very similar thermal stability, the onset decompositions of **P1**, **P2**, and **P3** are 402, 428, and 382°C under nitrogen atmosphere, respectively. Obviously, the thermal stability of the NDT-based polymers is adequate for their applications in PSCs.

Optical Properties of the Polymers

The UV-vis absorption spectra of **P1**, **P2**, and **P3** in toluene solution (5×10^{-5} mol L^{-1}) and of solid films are displayed in Figure 2, and the related data is summarized in Table I. The absorption range of the three polymers in solution are about 340 ~ 650 nm. In addition, the main absorption band of solid film is broader than that of in solution although both spectra show similar profiles. The absorption peaks of **P1**, **P2**, and **P3** of solid films are at 521 nm, 522 nm, and 531 nm, respectively. The absorption edges (λ_{onset}) of **P1** and **P2** are located at 644 nm, corresponding to optical band gap (E_g^{opt}) of 1.93 eV (E_g^{opt}=1240/λ_{onset}), while the λ_{onset} of **P3** is at 655 nm, corresponding to E_g^{opt} of 1.89 eV. As is well known, the optical absorption near the band edge follows the equation: $ahv=A(hv-Eg)^{n/2}$, in which a, v, A, and E_g are absorption coefficient, light frequency, proportionality constant, and band gap, respectively. In the equation, n decides the characteristics of the transition in a semiconductor (n=1, direct absorption; n=4, indirect absorption).[33,34] We also use Tauc plot[35] [$(ahv)^2$ versus hv plot] to obtain the E_g^{opt} of the three polymers, which were 2.02 eV, 2.02 eV, and 1.98 eV, respectively, as shown in Table I and Supporting Information Figure S3. Obviously, the E_g^{opt} of the three polymers obtained from both of the above two methods are closed to that of P3HT (1.9 eV).[36–39]

Electrochemical Properties of the Polymers

Electrochemical cyclic voltammetry (CV) is employed to measure the molecular energy levels of the three polymers. All potentials are reported versus Ag/AgCl with the ferrocene/ferrocenium couple used as an internal standard. The highest occupied molecular orbital (HOMO) and lowest unoccupied molecular orbital (LUMO) energy levels were calculated according to the empirical formulas: $E_{HOMO} = -(E_{ox}^{onset} + 4.4)$ (eV) and $E_{LUMO} = -(E_{red}^{onset} + 4.4)$ (eV).[40] As shown in Figure 3 and Table I, CV of **P1** depicted reversible reduction and oxidation behavior, from which a HOMO energy level of −5.20 eV and a LUMO energy level of −3.22 eV are deduced from the onset potentials, corresponding to an electrochemical band gap (E_g^{ec}) of 1.98 eV, which is quite close to the E_g^{opt} (1.93 eV) of **P1**.

Table I. Optical and Electrochemical Properties of P1, P2, and P3

	UV					CV				
	λ_{max} (nm)		λ_{onset} (nm)	E_g^{opt}		E_{ox}^{onset}	E_{red}^{onset}	HOMO	LUMO	E_g^{ec}
Polymers	Solution	Film	Film	[eV][a]	[eV][b]	[V]	[V]	[eV]	[eV]	[eV][c]
P1	520	521	644	1.93	2.02	0.80	−1.18	−5.20	−3.22	1.98
P2	530	522	644	1.93	2.02	0.76	−1.29	−5.16	−3.11	2.05
P3	527	531	655	1.89	1.98	0.85	−1.17	−5.25	−3.23	2.02

[a] Optical band gap, estimated from the absorption band edge of the polymer film, $E_g^{opt} = 1240/\lambda_{onset}$.
[b] Optical band gap, estimated from the Tauc plot [$(ahv)^2$ versus hv plot].
[c] Electrochemical band gap, E_g^{ec} = LUMO—HOMO.

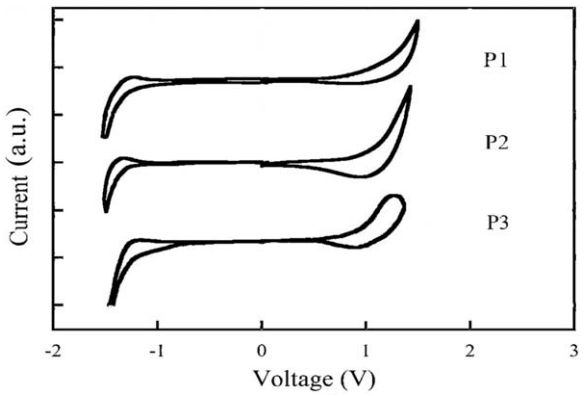

Figure 3. Cyclic voltammograms of P1, P2, and P3.

Similarly, based on the CV data, the HOMO and LOMO energy level of **P2** were −5.16 eV and −3.11 eV, **P3** were −5.25 eV and −3.23 eV, respectively. Thus, the obtained E_g^{ec} of **P2** and **P3** are 2.05 eV and 2.02 eV, which is also almost in good agreement with their optical bandgap. Compared with the HOMO level of P3HT (−5.0 eV),[41,42] the HOMO levels of the three polymers were lower. The open circuit voltage (V_{oc}) is proportional to the energy difference between the HOMO level of a polymer donor and the LUMO level of an acceptor.[43] Therefore, it is anticipated that the three polymers would attain higher V_{oc} in PSCs.

Photovoltaic Properties of the Polymers

To further explore the photovoltaic properties of the polymers, solar cell devices based on polymers blended with $PC_{61}BM$ were fabricated with a regular configuration of ITO/PEDOT : PSS/polymer : $PC_{61}BM$/Ca/Al. It is well known that the PCE is related to the short-circuit current density (J_{sc}) and the V_{oc} by: $PCE = \frac{Jsc\ Voc\ FF}{Psolar}$, where FF and P_{solar} are the fill factor and incident power from solar irradiation, respectively. The value of FF is the ratio of P_{max} ($=J_{MPP}V_{MPP}$) (P_{max}: the maximum power, J_{MPP}: the current density at the maximum power point, V_{MPP}: the voltage at the maximum power point) to the product of J_{sc} and V_{oc} ($FF=\frac{J_{MPP}\ V_{MPP}}{Jsc\ Voc}$). The solar cell characteristics were summarized in Table II. The blending weight ratios of polymers and $PC_{61}BM$ were varied from 1:1 to 1:3. It can be seen that the optimized polymer:$PC_{61}BM$ blend ratio weight for both **P1** and **P2**-based devices is 1:2, and for **P3**-based device is 1:3. It is worth to mention that the V_{oc} (0.62 ∼ 0.72 V) of the three polymers-based PSCs are higher than that (0.60 ∼ 0.62 V)[44] of P3HT-based device whatever the polymer : $PC_{61}BM$ ratio is. The higher V_{oc} of the three polymers-based PSCs should mainly be attributed to their lower HOMO levels compared with that of P3HT, as mentioned previously. Figure 4 presents the current–voltage (J–V) curves of the PSCs with optimized polymer:$PC_{61}BM$ blend ratio weight under illumination (AM 1.5G, 100 mW cm^{-2}). The related V_{MPP}, J_{MPP}, P_{max}, shunt resistance (R_{sh}), series resistance (R_s), and ideality factor (n) of the PSCs were summarized in Table SI and shown in Supporting Information Figure S4. In comparison with those of **P1** and **P3**-based device, V_{oc}, J_{sc}, and FF of **P2**-based device were increased to 0.72 V, 5.51 mA cm^{-2}, and 61.2%, giving an enhanced PCE of 2.43%. The incident photon-to-current conversion efficiency (IPCE) curves for the devices are given in Figure 5. It is clear that devices exhibited photo-response in the range of 340 ∼ 650 nm with IPCE range from 12 ∼ 46%. The

Table II. Performance of Solar Cells Based on P1/P2/P3 and $PC_{61}BM$

Polymers:$PC_{61}BM$	V_{oc} (V)	J_{sc} (mA cm^{-2})	FF (%)	PCE
P1:$PC_{61}BM$ (1:1)	0.66	2.58	53.4	0.91
P1:$PC_{61}BM$ (1:2)	0.66	4.96	56.8	1.86
P1:$PC_{61}BM$ 1:3)	0.62	4.66	49.8	1.44
P2:$PC_{61}BM$ (1:1)	0.70	2.78	57.4	1.12
P2:$PC_{61}BM$ (1:2)	0.72	5.51	61.2	2.43
P2:$PC_{61}BM$ (1:3)	0.68	4.70	52.6	1.68
P3:$PC_{61}BM$ (1:1)	0.66	2.40	43.5	0.69
P3:$PC_{61}BM$ (1:2)	0.66	2.87	51.8	0.98
P3:$PC_{61}BM$ (1:3)	0.64	4.63	54.3	1.61

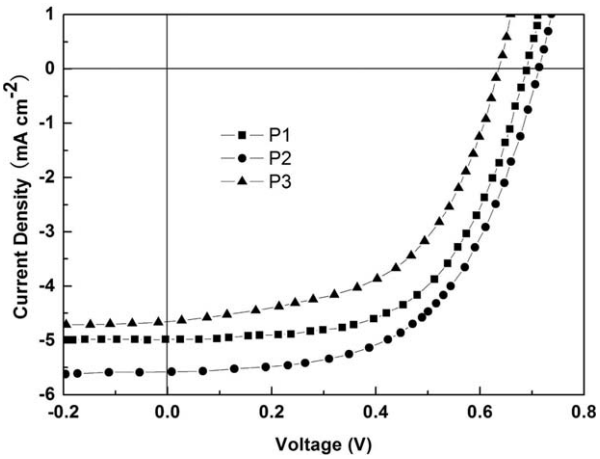

Figure 4. J–V characteristics of the PSCs with optimized polymer : $PC_{61}BM$ blend ratio weight based on P1, P2, and P3. The optimized polymer : $PC_{61}BM$ blend ratio weight for both P1 and P2-based devices is 1:2, and for P3-based device is 1:3.

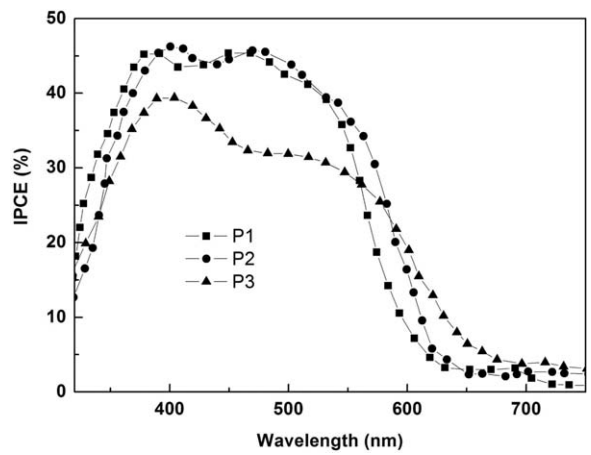

Figure 5. IPCE curves of the PSCs with optimized polymer : $PC_{61}BM$ blend ratio weight based on P1, P2, and P3.

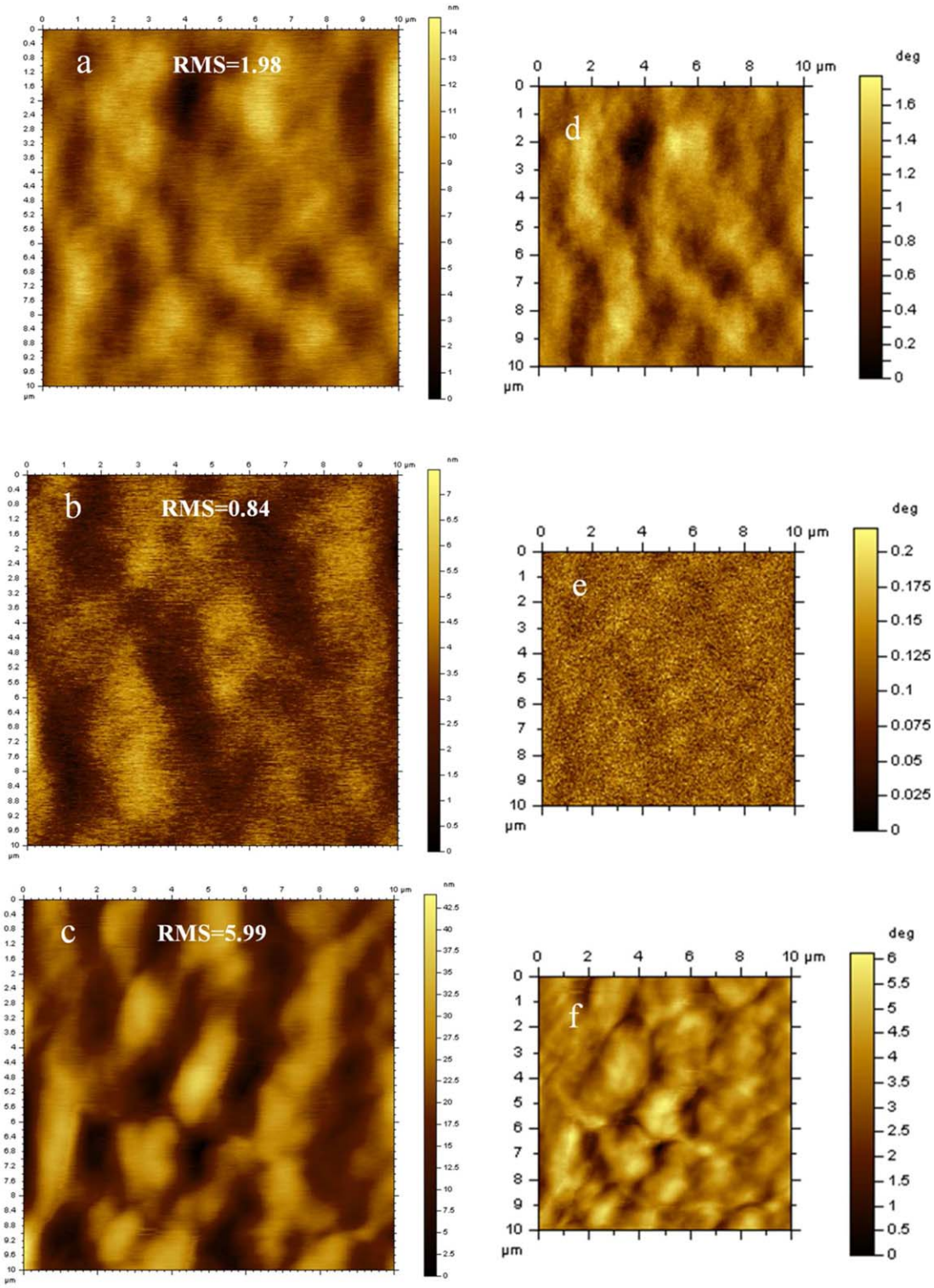

Figure 6. Tapping mode AFM height (a, b, and c) and phase (d, e, and f) images of 1 : 2 (weight ratio) composite film of P1 : $PC_{61}BM$, 1 : 2 (weight ratio) composite film of P2 : $PC_{61}BM$, 1 : 3 (weight ratio) composite film of P3 : $PC_{61}BM$, respectively. [Color figure can be viewed in the online issue, which is available at wileyonlinelibrary.com.]

profile of the IPCE plots is similar to the absorption spectra of the CPs, suggesting that all absorption wavelengths of the polymers contributed to photocurrent generation.

Atomic force microscopy (AFM) was used to characterize the surface morphology of the active layers. Figure 6 shows the typical height and phase images of the blend films. From the

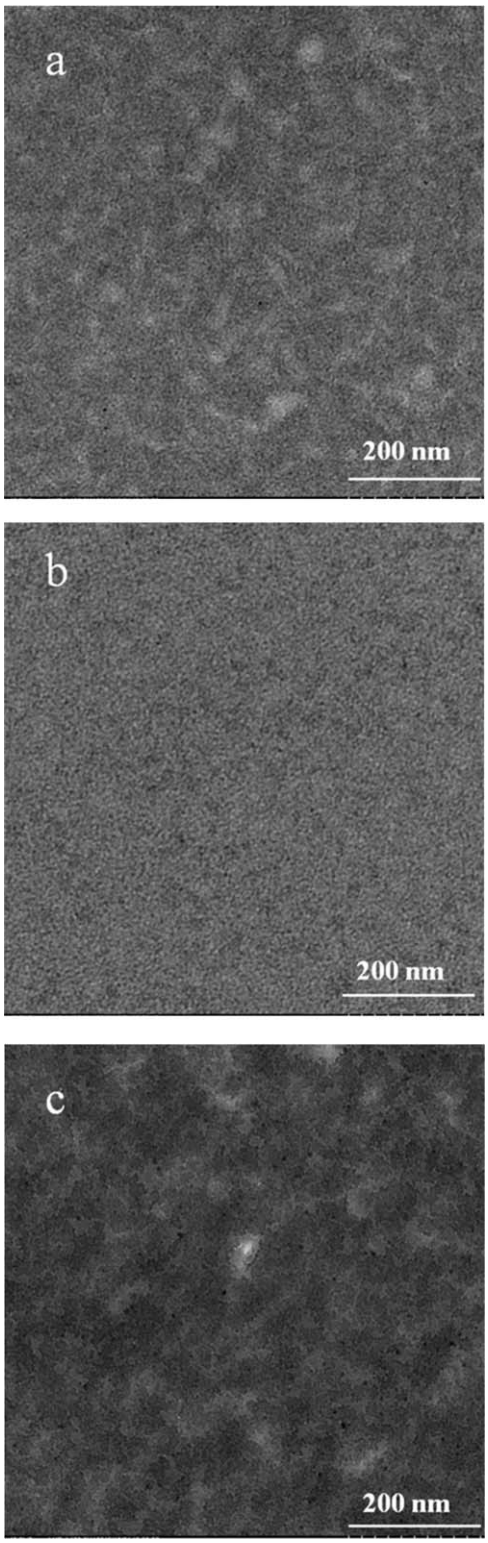

Figure 7. TEM images of 1 : 2 (weight ratio) composite film of P1 : $PC_{61}BM$ (a), 1 : 2 (weight ratio) composite film of P2 : $PC_{61}BM$ (b), 1 : 3 (weight ratio) composite film of P3 : $PC_{61}BM$ (c), respectively.

height images, the measured root-mean square (RMS) surface roughness values for **P1**, **P2**, and **P3**-based films were 1.98, 0.84, and 5.99 nm, respectively. From the phase images, clearly defined nanoscale phase separation is only observed in the **P2**-based film, the domains are not evenly distributed throughout the surface for **P1** and **P3**-based films. We also use transmission electron microscope (TEM) to characterize the vertical direction information of the active layers. As shown in Figure 7, the morphology of **P2**-based blend film is the most uniform and there is no large phase separation, indicating that formation of interpenetrating networks. Based on the above results, the improved morphology may be one of the reasons, which result in the highest FF and J_{sc} of P2-based PSCs.

Despite the fact that the V_{oc} of the three polymer-based PSCs outperform that of the devices based on P3HT/$PC_{61}BM$, the highest efficiency of 2.43% obtained in this article is still much lower than the optimized efficiency (around 4%) of the devices based on P3HT/$PC_{61}BM$.[44] We know, there are many factors that influence the efficiency of the PSCs, the efficiency around 4% of PSCs based on P3HT/$PC_{61}BM$ went through extensive optimization.[45,46] Therefore, the limited photovoltaic performance of the present devices could be further boasted by optimization of other device fabrication conditions except polymer : $PC_{61}BM$ blend ratio weight (for example, optimization of the annealing temperature and annealing periods of the polymer : $PC_{61}BM$ blend film, modification of electrodes, etc.), using mixed solvent mixtures or processing additives in the solutions of donor/acceptor blends and so on. Improvement of the solar cell performance is underway.

CONCLUSIONS

In conclusion, three medium bandgap CPs based on 10,11-di (2-hexyldecyloxy)dithieno[2,3-d:2′,3′-d′]naphtho[2,1-b:3,4-b′] dithiophene (NDT) have been prepared by Stille polycondensation reaction. The thermal, optical, electrochemical, and photovoltaic properties of the polymers were investigated in details. Prototype bulk heterojunction photovoltaic cells based on the blend **P1**/**P2**/**P3** and $PC_{61}BM$ show PCEs up to 1.61% ∼ 2.43% under 100 mW cm^{-2} illumination (AM1.5). Improvement of the solar cell performance and further employment of the CPs in the front cell in tandem PSCs are underway.

ACKNOWLEDGMENTS

This work was supported by the National Natural Science Foundation of China (No. 61404067, 61264002, 51463011, 61166002), the Natural Science Foundation of Gansu Province (No.: 1308RJZA159), the Program for New Century Excellent Talents in University of Ministry of Education of China (NCET-13-0840), the Research Project of Graduate Teacher of Gansu Province (2014A-0042), and Young Scholars Science Foundation of Lanzhou Jiaotong University (No.: 2014032).

REFERENCES

1. Gao, P.; Beckmann, D.; Tsao, H. N.; Feng, X.; Enkelmann, V.; Baumgarten, M.; Pisula, W.; Müllen, K. *Adv. Mater.* **2009**, 21, 216.
2. Takimiya, K.; Shinamura, S.; Osaka, I.; Miyazaki, E. *Adv. Mater.* **2011**, *23*, 4347.

3. Xiao, S.; Stuart, A. C.; Liu, S.; Zhou, H.; You, W. *Adv. Funct. Mater.* **2010**, *20*, 635.
4. He, F.; Wang, W.; Chen, W.; Xu, T.; Darling, S. B.; Strzalka, J.; Liu, Y.; Yu, L. *J. Am. Chem. Soc.* **2011**, *133*, 3284.
5. Wu, Y.; Li, Z.; Guo, X.; Fan, H.; Huo, L.; Hou, J. *J. Mater. Chem.* **2012**, *22*, 21362.
6. Yun, H. J.; Lee, Y. J.; Yoo, S. J.; Chung, D. S.; Kim, Y. H.; Kwon, S. K. *Chem. Eur. J.* **2013**, *19*, 13242.
7. Son, H. J.; Lu, L.; Chen, W.; Xu, T.; Zheng, T.; Carsten, B.; Strzalka, J.; Darling, S. B.; Chen, L. X.; Yu, L. *Adv. Mater.* **2012**, *25*, 838.
8. Xia, Y.; Li, Y.; Zhu, Y.; Li, J.; Zhang, P.; Tong, J.; Yang, C.; Li, H.; Fan, D. *J. Mater. Chem. C* **2014**, *2*, 1601.
9. Wang, B.; Tsang, S. W.; Zhang, W.; Tao, Y.; Wong, M. S. *Chem. Commun.* **2011**, *47*, 9471.
10. Lloyd, M. T.; Mayer, A. C.; Subramanian, S.; Mourey, D. A.; Herman, D. J.; Bapat, A. V.; Anthony, J. E.; Malliaras, G. G. *J. Am. Chem. Soc.* **2007**, *129*, 9144.
11. He, Z.; Zhong, C.; Su, S.; Xu, M.; Wu, H.; Cao, Y. *Nat. Photon.* **2012**, *6*, 591.
12. Kim, J. Y.; Lee, K.; Coates, N. E.; Moses, D.; Nguyen, T. Q.; Dante, M.; Heeger, A. *J. Science* **2007**, *317*, 222.
13. Sista, S.; Park, M. H.; Hong, Z.; Wu, Y.; Hou, J.; Kwan, W. L.; Li, G.; Yang, Y. *Adv. Mater.* **2010**, *22*, 380.
14. Chou, C.-H.; Kwan, W. L.; Hong, Z.; Chen, L. M.; Yang, Y. *Adv. Mater.* **2011**, *23*, 1282.
15. Dou, L.; You, J.; Yang, J.; Chen, C.-C.; He, Y.; Murase, S.; Moriarty, T.; Emery, K.; Li, G.; Yang, Y. *Nat. Photon.* **2012**, *6*, 180.
16. Jo, J.; Pouliot, J. R.; Wynands, D.; Collins, S. D.; Kim, J. Y.; Nguyen, T. L.; Woo, H. Y.; Sun, Y.; Leclerc, M.; Heeger, A. *J. Adv. Mater.* **2013**, *25*, 4783.
17. You, J.; Dou, L.; Yoshimura, K.; Kato, T.; Ohya, K.; Moriarty, T.; Emery, K.; Chen, C. C.; Gao, J.; Li, G.; Yang, Y. *Nat. Commun.* **2013**, *4*, 1446.
18. Kim, J. H.; Song, C. E.; Kim, B. S.; Kang, I. N.; Shin, W. S.; Hwang, D. H. *Chem. Mater.* **2014**, *26*, 1234.
19. Zhou, Q.; Hou, Q.; Zheng, L.; Deng, X.; Yu, G.; Cao, Y. *Appl. Phys. Lett.* **2004**, *84*, 1653.
20. Blouin, N.; Michaud, A.; Gendron, D.; Wakim, S.; Blair, E.; Neagu-Plesu, R.; Belletete, M.; Durocher, G.; Tao, Y.; Leclerc, M. *J. Am. Chem. Soc.* **2008**, *130*, 732.
21. Park, S. H.; Roy, A.; Beaupré, S.; Cho, S.; Coates, N.; Moon, J. S.; Moses, D.; Leclerc, M.; Lee, K.; Heeger, A. *J. Nat. Photon.* **2009**, *3*, 297.
22. Gilot, J.; Wienk, M. M.; Janssen, R. A. *J. Adv. Mater.* **2010**, *22*, E67.
23. Bijleveld, J. C.; Verstrijden, R. A. M.; Wienk, M. M.; Janssen, R. A. *J. Appl. Phys. Lett.* **2010**, *97*, 07330413.
24. Zou, Y.; Najari, A.; Berrouard, P.; Beaupré, S.; Aïch, B. R.; Tao, Y.; Leclerc, M. *J. Am. Chem. Soc.* **2010**, *132*, 5330.
25. Huo, L.; Guo, X.; Zhang, S.; Li, Y.; Hou, J. *Macromolecules* **2011**, *44*, 4035.
26. Whang, J. Y.; Hau, S. K.; Yip, H. L.; Davies, J. A.; Chen, K. S.; Zhang, Y.; Sun, Y.; Jen, A. K. Y. *Chem. Mater.* **2011**, *23*, 765.
27. Moon, J. S.; Jo, J.; Heeger, A. *J. Adv. Energy Mater.* **2012**, *2*, 304.
28. Shi, S.; Jiang, P.; Yu, S.; Wang, L.; Wang, X.; Wang, M.; Wang, H. L. Y.; Li, X. *J. Mater. Chem. A.* **2013**, *1*, 1540.
29. Zhao, X.; Yang, D.; Lv, H.; Yin, L.; Yang, X. *Polym. Chem.* **2013**, *4*, 57.
30. Gong, X.; Li, C.; Lu, Z.; Li, G.; Mei, Q.; Fang, T.; Bo, Z. *Macromol. Rapid Commun.* **2013**, *34*, 1163.
31. Baek, M. J.; Park, H.; Dutta, P.; Lee, W. H.; Kang, I. N.; Lee, S. H. *J. Polym. Sci. A: Polym. Chem.* **2013**, *51*, 1843.
32. Wang, K.; Zhao, Y.; Tang, W.; Zhang, Z. G.; Fu, Q.; Li, Y. *Org. Electron.* **2014**, *15*, 818.
33. Butler, M. A. *J. Appl. Phys.* **1977**, *48*, 1914.
34. Yi, Z.; Ye, J.; Kikugawa, N.; Kako, T.; Ouyang, S.; Stuart-Williams, H.; Yang, H.; Cao, J.; Luo, W.; Li, Z.; Liu, Y.; Withers, R. L. *Nat. Mater.* **2010**, *9*, 559.
35. Wood, D. L.; Tauc, J. *Phys. Rev. B* **1972**, *5*, 3144.
36. Koster, L. J. A.; Mihailetchi, V. D.; Blom, P. W. M. *Appl. Phys. Lett.* **2006**, *88*, 09351113.
37. Bundgaard, E.; Krebs, F. C. *Sol. Energy Mater. Sol. Cells* **2007**, *91*, 954.
38. Günes, S.; Neugebauer, H.; Sariciftci, N. S. *Chem. Rev.* **2007**, *107*, 1324.
39. Oliveira, E. F.; Camilo, A., Jr.; Silva-Filho, L. C.; Lavarda, F. C. *J. Polym. Sci. A: Polym. Chem.* **2013**, *51*, 842.
40. Li, Y. F.; Cao, Y.; Gao, J.; Wang, D. L.; Yu, G.; Heeger, A. *J. Synth. Met.* **1999**, *99*, 243.
41. Shrotriya, V.; Li, G.; Yao, Y.; Chu, C.; Yang, Y. *Appl. Phys. Lett.* **2006**, *88*, 07350813.
42. Ohori, Y.; Hoashi, T.; Yanagi, Y.; Okukawa, T.; Fujii, S.; Kataura, H.; Nishioka, Y. *J. Photopolym. Sci. Technol.* **2014**, *27*, 569.
43. Chen, J.; Cao, Y. *Accounts Chem. Res.* **2014**, *42*, 1709.
44. Tait, J. G.; Rand, B. P.; Heremans, P. *Org. Electron.* **2013**, *14*, 1002.
45. Chirvase, D.; Chiguvare, Z.; Knipper, M.; Parisi, J.; Dyakonov, V.; Hummelen, J. C. *J. Appl. Phys.* **2002**, *93*, 3376.
46. Boland, P.; Sunkavalli, S. S.; Chennuri, S.; Foe, K.; Abdel-Fattah, T.; Namkoong, G. *Thin Solid Films* **2010**, *518*, 1728.